

Migration Characteristics of Some Chemical Species in a Granite Fracture according to their Chemical Properties

Chung-Kyun Park[†], Bo-Hyun Ryu and Pil-Soo Hahn

Korea Atomic Energy Research Institute, Research Team of High Level Radioactive Waste Disposal, Daejeon 305-353, Korea

(Received 25 October 2001 • accepted 18 June 2002)

Abstract—Migration experiments were carried out in artificial rock fractures of 50×50 cm scale in order to understand the transport phenomena of contaminants in deep geological environment. The tracers used in this experiments were tritiated water, anion, polymers, and sorbing cations. The experimental study was focused on the interpretation of the retardation and matrix diffusion of the tracer in the fracture. To visualize migration phenomena, an organic dye, eosine, was used as a tracer. The migration plumes were taken with a digital camera as a function of time and stored as a digital image file. Computer simulation was performed not only for the hydraulic behavior such as distributions of pressure and flow vectors in the fracture but also for the migration plume and the elution curves. These simulation results were interpreted by comparing experimental ones, thus providing a way to understand migration behavior of tracers and interaction between rock and chemical species.

Key words: Migration, Sorption, Retardation, Matrix Diffusion, Random-walk Method

INTRODUCTION

Flow and migration through rock fractures has become an important field of study in contaminant transport. Fractures in rocks tend to dominate the hydraulic behavior, particularly when the rock matrix is of low permeability. Individual fractures act as conduits through the media and allow free passage between the matrix blocks which bound the fracture. Flow and transport in a rock fracture have been considered previously in some of laboratory experiments [Moreno et al., 1985; Keum et al., 1997; Park et al., 1997]. Recently, transparent fractures have been used to study various flow processes [Gentier et al., 1989; Wan et al., 1999]. Transparent fractures can be designed and fabricated with varying aperture in a range of probable structures or be cast from individual natural fractures in epoxy or glass to yield a realization of nature. Similarly, we used an acrylate plate to simulate the fracture system for the observation of migration plumes of organic dye in the fracture. Such visible images of migration plume in the analog fracture may give important suggestions and information in understanding the invisible migration plume in the rock fracture.

In this study, we focused on physicochemical interactions between rock and chemical species. Thus, we designed a simple fracture system having a pair of parallel plates. In order to describe the fluid flow in the fractured rock, we make the assumption that each fracture is idealized as a pair of parallel plates separated by a constant distance which represents the aperture of the fracture. The processes to be considered are advection, dispersion, and sorption in the fracture plane, coupled with diffusion of the tracer into the stagnant pores in the rock matrix. These last two processes can be significant processes for retarding the migration of tracers. Crystalline rocks such as granite have very low porosity of 0.2-0.5% but the

total pore volume is large compared to that of the fracture surface. For a block of granite with volume of 1,000 l and a connected porosity of 0.3%, the total accessible pore volume is 3 l. Thus diffusion into the rock mass in the fracture surface was treated as an important study topic in this experiment. For this work, we compared migration characteristics of tracers according to their chemical properties: water, anion, sorbing cation, and polymers.

We are also going to develop a generic model describing the migration of the tracers in various rock fractures, that is, to develop a variable aperture channel model for characterizing the fracture plane including a constant aperture fracture. And a particle tracking scheme is applied for the solute transport. We will present our investigations of the flow and migration in two-dimensions, representing the physical situation of the experimental setup. By solving the numerical model for the flow and transport of some typical tracers in various assumptions, we attempt to understand the flow characteristics and to identify the key parameters that control the migration pattern, thus providing a way to interpret the fracture field and the interactions between rock and chemical species.

TRANSPORT MODEL

1. Flow Field in the Rock Fracture

The fracture plane may be subdivided into imaginary subsquares. The fluid flow through the fracture is then calculated for a constant injection/withdrawal rate as well as for constant pressure conditions. For a constant laminar flow, the volumetric flow rate through a parallel fracture may be written as:

$$Q = \frac{1}{12\mu} \frac{b^3 W}{L} \Delta P \quad (1)$$

where ΔP is the pressure drop over a length of L and W and μ is the viscosity. Eq. (1) may be applied to each of the subsquares enclosed by the grid lines. When the volumetric flow rate from node

[†]To whom correspondence should be addressed.

E-mail: ckpark@kaeri.re.kr

i to node j is Q_{ij} , the volumetric flow rate can be rewritten

$$Q_{ij} = C_{ij} (P_i - P_j) \quad (2)$$

where P_i is the pressure at node i, Node i implies an index of the i th subsquare in the fracture surface. C_{ij} is the flow conductance between nodes i and j.

$$C_{ij} = \left[\frac{b^3 \Delta y}{12 \mu \Delta x} \right] \quad (3)$$

where Δx and Δy are the length of x and y coordinate in a subsquare, respectively.

The mass balance at each node may be written as:

$$\sum_j Q_{ij} = \sum_j C_{ij} (P_i - P_j) = E_i \quad (4)$$

where E_i is the injection rate or withdrawal rate at node i. The subscript j stands for the four facing nodes of surrounding subsquares to node i.

Except for the nodes at the boundaries, the pressure at each node is unknown to be solved with the Gauss-Seidel iteration method. The flow between adjacent nodes can be calculated using Eq. (4). After flow vectors are obtained at all nodes, solute transport can be simulated in this flow field.

2. Random-walk Particle Tracking Metho

A two-dimensional random-walk particle tracking algorithm is used to simulate the solute transport through the flow fields. Particle displacements in each time step consisted of an advective displacement based on local velocities calculated by using the pressure field and random diffusive displacement. Particles, which are representing the mass of a solute contained in a defined volume of fluid move through a fracture with two types of motion. One motion is with the mean flow along stream lines and the other is random motion, governed by scaled probability [Desbarats, 1990; Washburn et al., 1980].

At the inlet, a certain amount of particles were introduced; in this study, 10,000 particles are used and distributed at each node between flow channels with a probability proportional to the flow rates. Particles are then convected by discrete steps from node to node until they reach the outlet node at which point the arrival time is recorded. This procedure is repeated for all of particles to get a stable probability distribution. The residence time for nonsorbing tracers in a given subsquare is determined from the total flow through that subsquare and its volume. The residence time of a particle along each path is obtained as the sum of the residence times in all subsquares through which the particle had passed. Four transport processes are considered in modelling the solute transport: advection

(V), hydrodynamic dispersion (D), diffusion into the rock mass (D_e), and sorption (K_a).

EXPERIMENTAL

1. Experimental Setups

A block of Hwangdeung granite with dimensions of $50 \times 50 \times 10$ (cm) containing an artificial open fracture was prepared. The mineralogical and chemical composition of the granite are listed in Tables 1 and 2, respectively. In Table 1, a little amount of secondary minerals can be observed, which means that this rock is a little weathered. Also this rock has an interconnected porosity of 0.37% with the specific gravity of 2.55.

Two kinds of experimental setups having same dimensions of $50 \times 50 \times 10$ (cm) were prepared. The setup I is designed for taking the images of the migration plume and this analog fracture is fabricated by holding an acrylate as the upper plate and granite as the lower one in close contact. When a tracer migrates through the gap between the acrylate and the granite, the migration plume can be observed through the transparent acrylate plate. The setup II has granite blocks for both plates and is intended to study interactions between rock and chemical species. The setup was assembled by placing the fracture plates in contact and bolting the frames together to a uniform torque. The outer gap of the fracture was sealed with a silicone adhesive to prevent from leaking of fluid. Stainless steel frames were mounted on both halves of the block and connected to each other by four threaded rods and bolts. Two boreholes on the upper plate are selected as the inlet and the outlet for transporting of fluid. Before the migration test, gases in the rock fracture were evacuated and the rock block was submerged in the water container to be saturated with water. The water in the container kept almost a constant temperature of 20 °C.

2. Migration Experiments

Four kinds of chemical species were used for migration test: (1) tritiated water (THO), (2) anion; Cl⁻ & Br⁻, (3) polymeric organic dye; NaLS (sodium lignosulfonate, M_w=24,000) and Eosine (C₂₀H₆Br₄Na₂O₅, M_w=691), and (4) sorbing cation; Sr²⁺ & Cu²⁺. The aliquot solution of 1.2 ml containing tracers was injected as a band input function into the inlet borehole in separate campaigns, fed with a HPLC pump through the fracture at a flow rate of 0.5 ml/min and collected at the outlet borehole as shown in Fig. 1. The eluted solution was collected by using a fraction collector.

The flow was directed along the gap of the fracture through implementation of no-flow boundaries along the fracture sides. The fluid was uniformly supplied to the inlet hole by using an HPLC pump, creating a constant flow boundary condition. At the down-

Table 1. Mineralogical composition of the granite

Mineral	Quartz	Plagioclase	K-feldspar	Biotite	Hornblende	Sphene	Opaque
%	45.8	24.2	12.4	12.5	2.2	0.4	1.2

Table 2. Chemical composition of the granite

Element	SiO ₂	Al ₂ O ₃	Fe ₂ O ₃	TiO ₂	MgO	CaO	Na ₂ O	K ₂ O	MnO
%	72.54	13.47	2.99	0.40	0.91	2.20	3.28	3.59	0.06

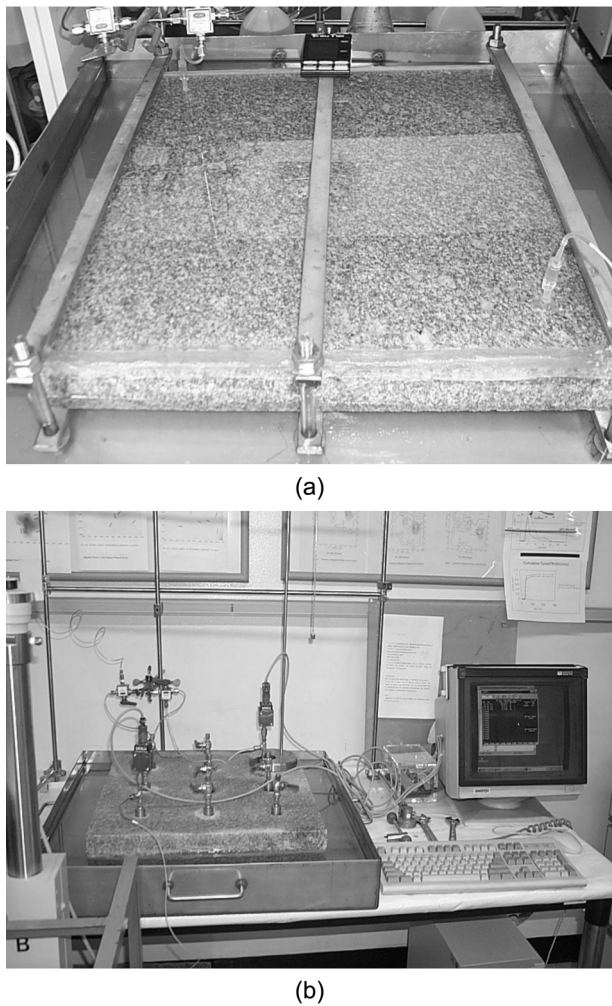


Fig. 1. Two kinds of experimental setups for migration test.

(a) Setup I: Transparent Fracture Analog, upper plate: acrylate, bottom plate: granite [50×50×5.5 (cm)]
 (b) Setup II: Artificial Fractured Granite, upper plate: granite, bottom plate: granite [50×50×10 (cm)]

stream end of the fracture, a constant head boundary was implemented. In particular, Eosine, an organic dye, was used to visualize the migration plume in the flow plane of the setup 1. The migration plumes were taken with a digital camera as a function of time and stored as a digital image file.

The concentrations of eosine and NaLS were analysed with the UV/VIS spectrophotometer at the wavelength of 524 nm, 282 nm, respectively. The concentrations of Cl^- and Br^- were analysed with the ion electrodes of Orion Research Inc. Sr^{+2} and Cu^{+2} were analysed with the ICP-MS. THO was analysed with a Liquid Scintillation Counter.

3. Hydraulic Properties in the Fracture

The fracture surface was divided into an imaginary matrix of 20×

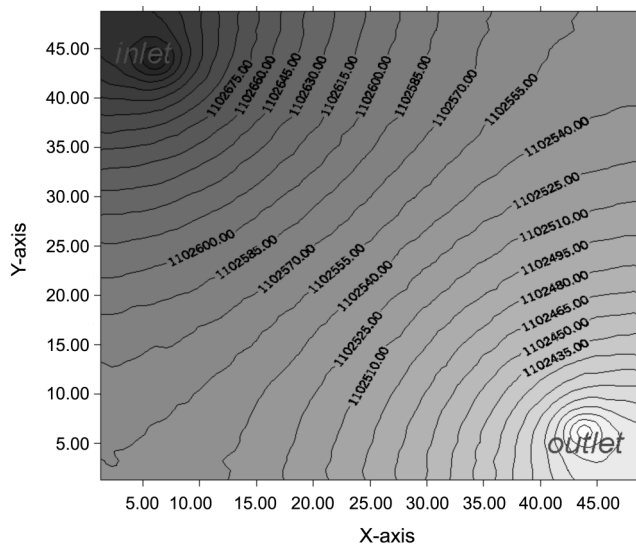


Fig. 2. Simulation result of pressure distribution in the fracture.

20 sub-squares. All sub-squares were assigned the same aperture value. Recall that the boundary conditions employed to solve the flow through the system are the constant head boundary condition, that is, the injection node is at the higher constant pressure P_1 and the withdrawal node is at the lower constant pressure P_2 . The flow between adjacent nodes can be calculated by using Eq. (2). The pressure distribution in the field was simulated with a graphic program SURFER as shown in Fig. 2. The pressure drop, ΔP , between the inlet and the outlet were about 48 N/m² and 280 N/m² in setup I & II, respectively. Then the aperture could be calculated with the ΔP and Eq. (1), and was arranged in Table 3. The difference of pressure drop between two setups is probably due to the differences of aperture size and the viscosity of media. The heavier load of the upper plate in the setup II may squeeze more intensively the aperture width than that in the setup I.

Fig. 3 showed two dimensional flow field and some examples of supposed stream traces, which was plotted with a commercial program TECPLOT. Figs. 2 and 3 show symmetric trends in the distributions of the pressure and the flow vector pivoting the diagonal line between the inlet and the outlet. At the edges of both sides of the fracture, the flow vectors were very small, and thus the flow was regarded as almost stagnant.

4. Batch Sorption Test

To calculate the amount of the tracer sorbed on the fracture surface, a sorption test was carried out in a batch. Granite blocks were in contact with water for a month to get a pre-equilibrium between the two phases before a sorption experiment was carried out. A small drilled core sample of the granite and 1,000 ml of water were prepared in a PE flask with a cap. Sorbing tracers were added in the flask at a certain time. The flask was shaken in a water bath at 20 °C for a month. Five ml of the contacted solution was sampled at an

Table 3. Experimental setups and parameter values

Experimental	Setup	Type of experiment	Weight of upper plate [g]	ΔP [N/m ²]	b (calculated) [cm]
Setup I	Rock-acryl	Migration plum	1,500	480	0.028
Setup II	Rock-rock	Elution curve	2,700	2,800	0.011

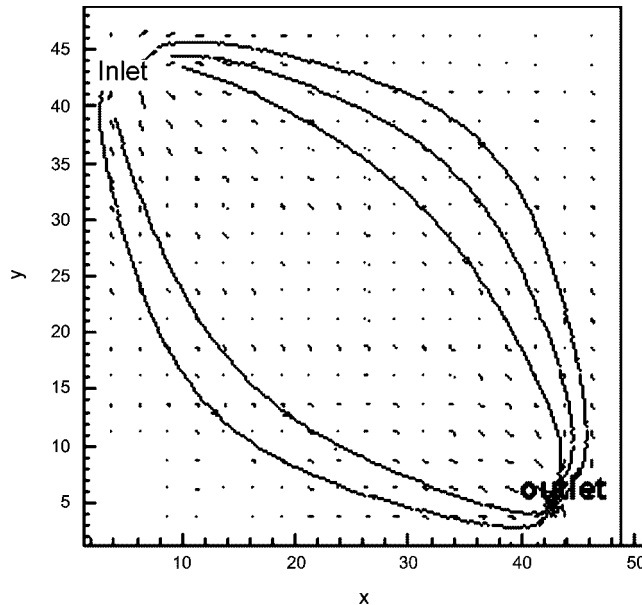


Fig. 3. Distribution of flow vectors in flow field and some examples of stream tracers, the size of the arrow is proportional to the magnitude of the flow rate.

appropriate time interval and centrifuged for 20 minutes at 3,000 rpm. And the concentration of the supernatant solution was measured with the ICP-MS. The distribution coefficient based on the specific surface area of the media, K_a , was calculated by the following equation:

$$K_a = \frac{C_0 - C}{C} \cdot \frac{V}{S_a} \quad (5)$$

where, S_a : specific surface area of the rock, C_0 : initial concentration of the tracer, C : final concentration of the tracer, V : volume of the solution in the batch container.

The concentrations of the tracers in the batch solution decrease rapidly within 20 hours and slowly go down afterwards with a time scale of weeks. When the rate of concentration change becomes negligible, the sorption system is assumed to be at a quasi-equilibrium state. Thus this sorption system may be divided into two stages for convenience. At the initial stage, tracers may sorb mainly on the outer surface of the rock and at the later stage the tracers penetrate through the micropores of the rock to the inner surface of the rock. Diffusion process would be the rate-controlling step of this later stage [Park et al., 1992; Skagius, 1982]. The values of K_a were 0.07 and 0.23 for Sr and Cu, respectively.

5. Migration Plumes of Nonsorbing Tracer

The migration plume of the organic dye, eosine, in the setup I was taken with a digital camera as a function of time and shown in Fig. 4. The migration plume did not follow a linear trace along the diagonal direction between the inlet and the outlet, but moved across the full width of the fracture as a two dimensional span around the diagonal line. Thus a two-dimensional migration model is required to describe this migration plume and, needless to say, it is difficult to apply one-dimensional model. Comparing these results with the simulated one in Fig. 5, the general trend of each was consistent. In this simulation, matrix diffusion of eosine in both fracture sides was ignored. Though the simulated migration plume showed per-

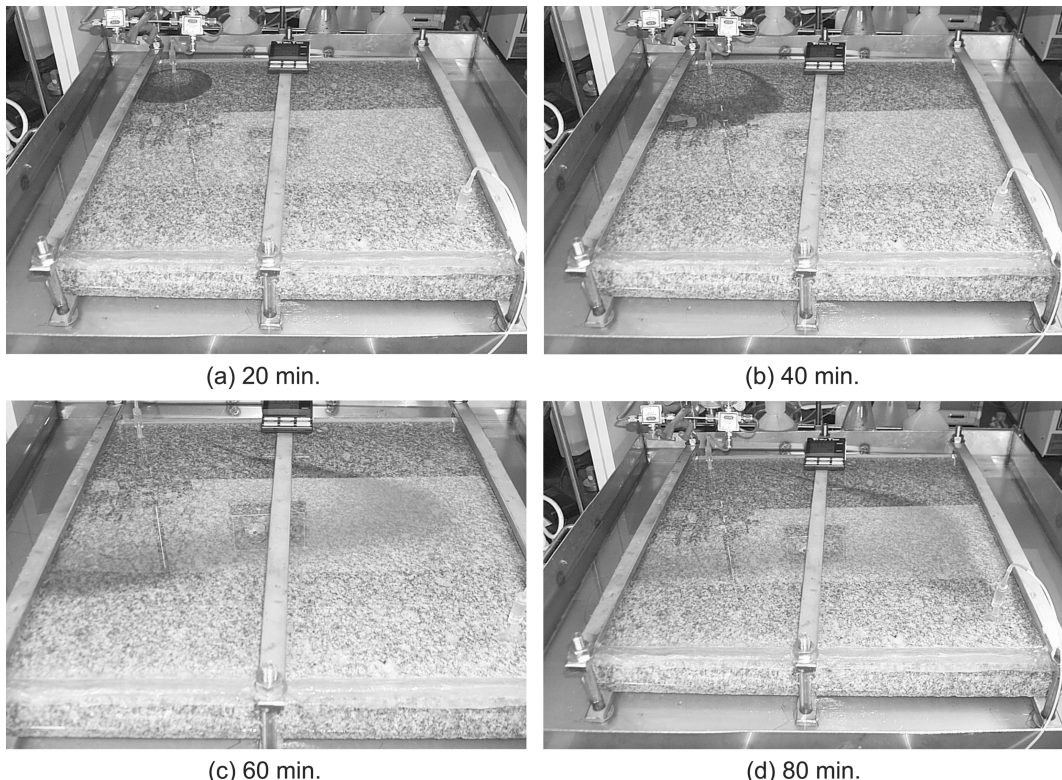


Fig. 4. Migration plume of eosine in the analog fracture as a function of time.

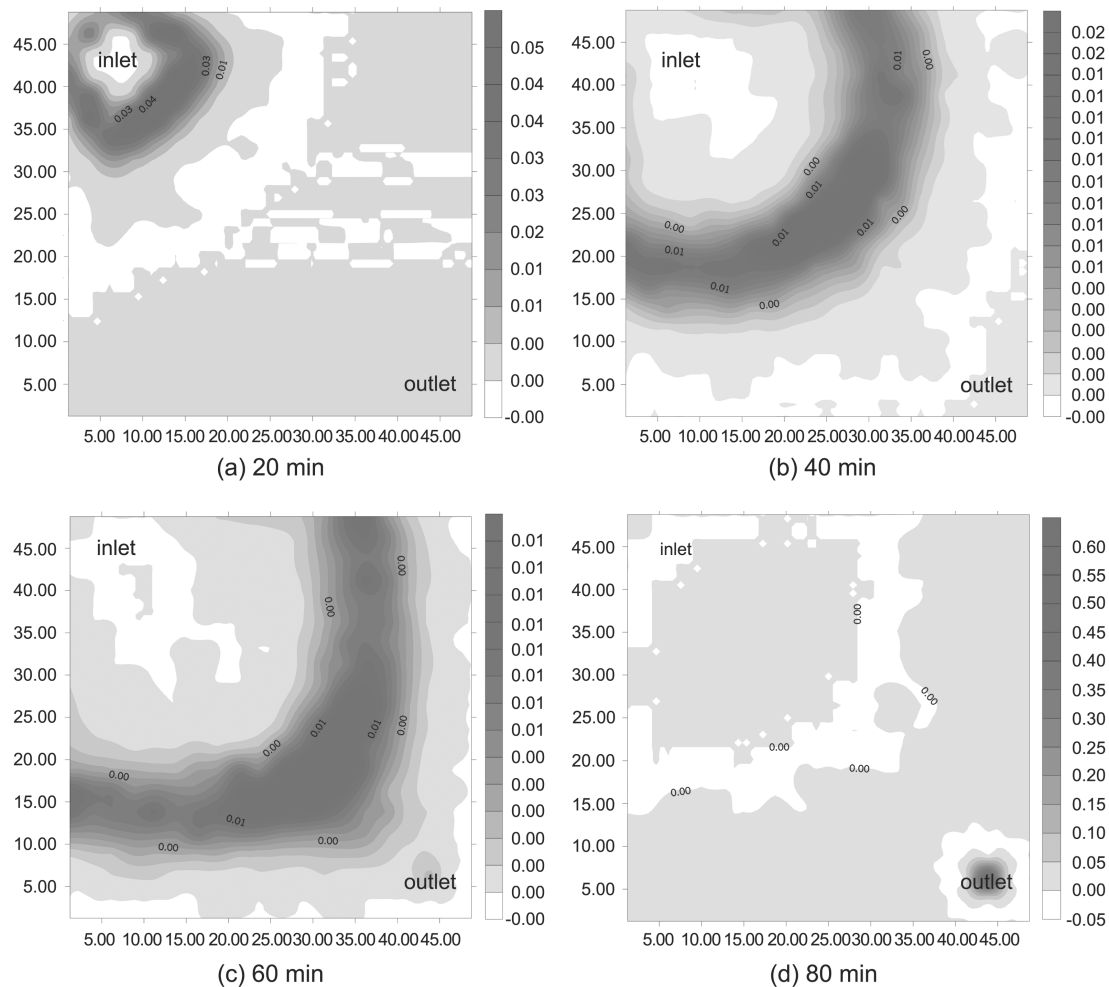


Fig. 5. Simulated contours of migration plume in the fracture with time.

fect symmetric fan-shape around the diagonal line, the experimental one did not show symmetric shape at later stage. It seems to be due to the discrepancy between the experimental setup and model assumption of the constant aperture. Near the outlet of the setup II there might be some variation of aperture value, which showed irregular shape of migration plume at later stage. Because the flow is proportional to the cube of the aperture, even the smallest change of the aperture can give large effect on the migration plume.

6. The Elution Curve and Retardation

A brief summary on the simulation procedures for obtaining elution curves is as follows:

- (1) At a given node, calculate the volumetric flux across each four faces of the surrounding grid cell as in Rq. (2). Q_{ij} ($j=1, 2, 3, 4$)
- (2) Calculate the total outflow from the subsquare.

$$Q'_i = \sum_{j=1}^4 Q_{ij}$$

- (3) Assign a probability to each of the four possible flow directions. Inflow directions receive a probability of zero. Outflow directions receive a probability equal to their fraction of the total outflow from the subsquare.

$$p_{ij} = Q_{ij} / \sum_{j=1}^4 Q_{ij}$$

(4) Generate random number and choose an outflow direction according to the discrete probability distribution.

(5) Move particle to the next node in the selected direction at a velocity equal to the total outflow rate from the subsquare. This ensures conservation of total mass flux through the subsquare at any given particle step and, over many passages, conservation of mass flux in each direction.

(6) Increment the cumulative travel time by the appropriate amount.

$$t_{cum} = \sum_{i=1}^n t_i$$

(7) Repeat the above steps until the particle arrives at the withdrawal point.

This procedure is repeated for a specified number of particles to get a stable probability distribution.

The simulated and experimental elution curves of the tracer are shown together in Fig. 6. When advection, sorption, hydrodynamic dispersion and diffusion into the rock mass are considered, different particles in the same subsquare will have different residence times.

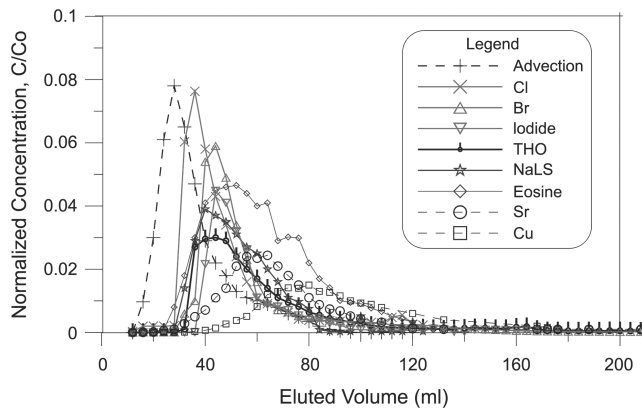


Fig. 6. Calculated and experimental elution curves of the tracers.

The residence times for these particles can be expressed as a probability density function, which in turn can be regarded as the elution concentration of a pulse injection. Integrating this curve over time gives a cumulative elution profile as shown in Fig. 7. In general, the cumulative elution curves of tracer transport in two dimensions through those flow field have a fast rise at early times, since the majority of the particles take the fastest flow paths; then there is a long tail in the breakthrough curve due to a small fraction of particles meandering through the fracture with small volumetric flow rates. The characteristic values of the simulated curves were arranged in Table 4, but the only one curve for the advection process was shown in Figs. 6 and 7 avoiding complication among curves.

If the gap of the fracture is assumed as a thin cube, the aperture of the fracture can be estimated from the elution curve of nonsorbing tracer and from the mass balance in the fracture by Eq. (6).

$$LW (b/\tau) = Q \quad (6)$$

where, τ : peak arriving time of the elution curve.

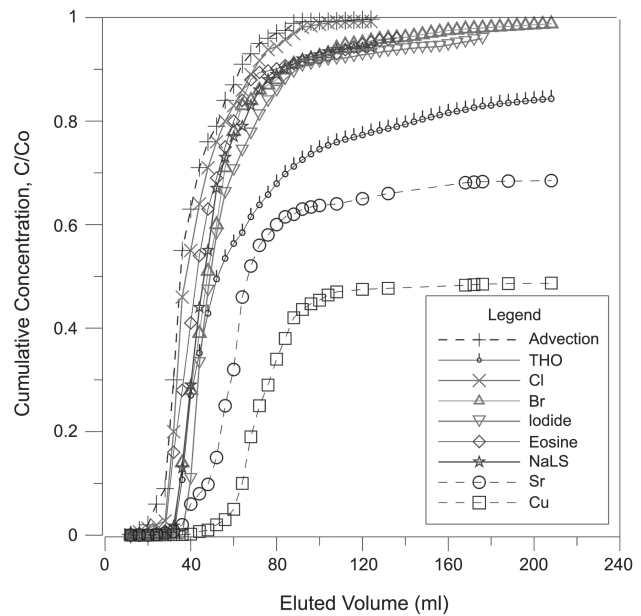


Fig. 7. Calculated and experimental cumulative elution curves of the tracers.

The above equation can be rearranged,

$$b = (Q/LW) \tau \quad (7)$$

The calculated b was 0.016 cm. It gives resonable correspondence with the simulated result of 0.011 cm using the pressure difference of 280 N/m² between the inlet and the outlet as shown in Fig. 3. While linear velocity in the fracture is expressed as,

$$u = Q/(W \cdot b) \quad (8)$$

The obtained value of u is 0.63 cm/min. In Fig. 6, residence time of nonsorbing tracer in the fracture are approximately 80 minutes,

Table 4. Characteristics of the elution curves of the tracers

Tracer	Retention time		Peak height C/Co	Retardation factor		Recovery	
	τ (min, ml)			Migration	Sorption	%	at t (min)
Simulation							
V (advection) ¹	56	28	0.079	0.67	-	100	480
V+Ds ²	60	30	0.058	0.71	-	100	480
V+Ds+De ³	70	35	0.08	0.9	-	<100	420
Experiment							
THO	80-90	40-45	0.03	1	1	83	420
Cl ⁻	70	35	0.075	0.83	1	100	480
Br ⁻	84	42	0.058	≈1	1	99	420
I ⁻	90	45	0.045	≈1	1	96	380
Eosine	80-12	40-60	0.047	≈1	1	96	240
NaLS	80	40	0.04	≈1	1	97	240
Sr ²⁺	100-140	50-70	0.026	1.2-1.7	7.4	54	420
Cu ²⁺	140-180	70-90	0.017	1.7-2.1	21.9	43	420

*¹: Simulation when only advection process is considered.

*²: Simulation when the advection and hydrodynamic dispersion are considered.

*³: Simulation when advection, dispersion and matrix diffusion are considered.

$$D_e = 3.7 \times 10^{-7} \text{ cm}^2/\text{m}$$

or as eluted volume, 40 ml. If the tracer follow a linear trace along the diagonal line of 43 cm long between the inlet and the outlet, then the aperture should be larger than 0.1 cm to get the travel time about 80 min; that would be an unreasonably large value of the aperture. Therefore, the tracer did not across the straight line of the shortest course, but moved as a two-dimensional fan-shape as shown in Fig. 4.

To analyze the migration characteristics of tracers according to their chemical properties, the elution curves and the cumulative elution curves were examined in Figs. 6 and 7. In these curves, the tritiated water was regarded as a basic tracer because it has the same chemical properties with the water. Usually, tritium, anion, and some organic dye are assumed as the nonsorbing tracer. Therefore, in modeling work, it is commonly assumed that the distribution coefficient, $K_a=0$, and the retardation factor, $R=1$, for such nonsorbing tracers. However, in this experiment, they showed different migration behavior. The anions and polymeric organic dyes migrate faster than the tritium in the natural fracture and they are recovered almost 100% at the exit; whereas tritium was recovered only 83%. This phenomenon can be explained in two aspects. First, because the surface of the rock fracture is negatively charged, the anion could be expelled by the rock surface and thus cannot access to the pore by the anion exclusion effect [Langmuir, 1997]. Second, the ionic size of the polymeric organic dye is larger than cations by over 1,000 times. And the size of the micropores of the rock ranges from micrometer to subnanometer. Considering that the ionic size of the cation is about several Å, cations and water molecule can penetrate easily into the micropore of the rock, while the polymeric substances cannot. Therefore, it could be concluded that tritium diffuses into the rock pores, but anions and polymeric tracers hardly diffuse into the rock matrix.

The migrating sorbing tracer interacts with the fracture surface and it retards as much as their sorption capacity. The degree of retardation is usually expressed as the retardation factor, R

$$R = \frac{\tau_n}{\tau_w} = \frac{u_w}{u_n} = 1 + \frac{K_a}{b} \quad (9)$$

where, τ_n : tracer travel time, τ_w : water travel time, u_w : water velocity, u_n : tracer migration velocity.

The calculated R values from the elution curves are arranged in Table 4, while R can also be presumed from batch sorption data by Eq. (9) and the results are also arranged in Table 4. The R values from the elution curve was smaller than the R values from the sorption data. It seems that the sorbing tracers did not interact sufficiently with the rock surface in the flow rate of 0.5 ml/min.

CONCLUSION

The chemical species showed different migration characteristics in the rock fracture according to their chemical properties. The anions such as Cl^- , Br^- and I^- and the polymeric dyes such as NaLS and eosine did neither interact chemically with the rock, nor penetrate into the micropores of the rock due to the anion exclusion and the size hindrance, respectively. While the tritiated water diffused into the rock pores and 17% of the injected remained in the rock mass. The sorbing cations, Sr and Cu, did not retard as much as the expected from the batch sorption data. It seems that the sorbing tracers did not fully interact with the rock surface in the flow rate

of 0.5 ml/min or this system did not reach an equilibrium state like the batch system.

The tracers moved as two-dimensional span rather than one-dimensional straight line course between the inlet and the outlet in this fracture system. The migration plume through fracture taken with a digital camera corresponded to the results of model simulation reasonably. The combination of the experimental observation and the model simulation gave good suggestions to further understand the flow and transport in the rock fracture.

NOMENCLATURE

b	: fracture aperture
C	: concentration of the tracer
C_{ij}	: flow conductance between nodes i and j
E_i	: injection rate or withdrawal rate at node i
h	: hydraulic head
K_a	: distribution coefficient based on the specific surface area of the media
P_i	: pressure at node i
p_{ij}	: probability of the flow from node i to node j
Q_{ij}	: volumetric flow rate between nodes i and j
R	: retardation factor
S_a	: specific surface area
t_i	: residence time of a particle in node i
t_{cum}	: cumulative travel time of a particle along the flow path
u	: linear velocity of the tracer in the fracture
V	: volume of the solution in the batch container
τ	: residence time in the fracture
μ	: viscosity of the transport solution

REFERENCES

Anderson, M. P. and Woessner, W. W., "Applied Groundwater Modeling," chap. 11, Academic Press (1992).

Bear, J., "Hydraulics of Groundwater," McGraw-Hill (1979).

Desbarats, A. J., "Macrodispersion in Sand-Shale Sequences," *Water Resour. Res.*, **26**(1), 153 (1990).

Gentier, S., Billaux and van Vliet, "Laboratory Testing of the Voids of a Fracture," *Rock Mech. Rock Eng.*, **22**, 149 (1989).

Keum, D. K., Park, C. K., Hahn, P. S. and Vandergraaf, T., "A Stratified Channel Model with Local Longitudinal Dispersion," *Nucl. Tech.*, **120**, 211 (1997).

Langmuir, D., "Aqueous Environmental Geochemistry," Chap. 3.5, Prentice-Hall (1997).

Moreno, L., Neretnieks, I. and Eriksen, T., "Analysis of Some Laboratory Tracer Runs in Natural Fissures," *Water Resour. Res.*, **21**(7), 951 (1985).

Moreno, L., Tsang, C. F., Hale, F. V. and Neretnieks, I., "Flow and Tracer Transport in a Single Fracture," *Water Resour. Res.*, **24**, 2033 (1988).

Moreno, L. and Neretnieks, I., "Flow and Nuclide Transport in Fractured Media," *J. of Contam. Hydro.*, **13**, 49 (1993).

Park, C. K., Keum, D. K. and Hahn, P. S., "Stochastic Analysis of Contaminant Transport Through a Rough-surfaced Fracture," *Korean J. Chem. Eng.*, **12**, 428 (1995).

Park, C. K., Vandergraaf, T. T., Drew, D. J. and Hahn, P. S., "Analysis

of the Migration of Nonsorbing Tracers in a Natural Fractures in Granite using a Variable Aperture Channel Model," *J. of Cont. Hydrol.*, **26**, 97 (1997).

Park, C. K. and Hahn, P. S., "Effects of Aperture Density Distribution on the Flow Through a Rock Fracture with Line-source and Line-collection," *J. of Kor. Nucl. Soc.*, **30**(6), 485 (1998).

Park, C. K. and Hahn, P. S., "Reversibility and Linearity of Sorption for Some Cations onto a Bulguksa Granite," *Korean J. Chem. Eng.*, **16**, 758 (1999).

Tsang, Y. W., Tsang, C. F., Neretnieks, I. and Moreno, L., "Flow and Tracer Transport in Fracture Media- A Variable-Aperture Channel Model and its Properties," *Water Resour. Res.*, **24**(12), (1988).

Washburn, F. E., Kaszeta, C. S., Simmons, and Cole, C. R., "Multicomponent Mass Transport Model," PNL-3179 (1980).

Wan, J., Tokunaga, Tsang, and Bodvarsson, G., "Improved Glass Micromodel Methods for Studies of Flow and Transport in Fractured Porous Media," *Water Resour. Res.*, **32**, 1955 (1996).

Yamashita, R. and Kimura, H., "Particle-Tracking Technique for Nuclide Decay Chain Transport in Fractured Porous Media," *J. of Nuclear Sci. and Tech.*, **27**, 1041 (1990).